Journal of Power Sources, *25* (1989) 61 - 74

RELIABILITY OF COMMERCIAL LITHIUM BUTTON CELLS
II. EFFECT OF THE STATE-OF-DISCHARGE AND ENVIRONMENT ON THE PASSIVATION RESISTANCE

JEAN-PAUL RANDIN

ASULAB SA, Research Laboratories of the SMH Group, Passage Max-Meuron 6, CH-2001 Neuchâtel (Switzerland)

(Received March 4, 1988; in revised form August 11, 1988)

Summary

The passivation resistance of commercial Li/MnO_2 and Li/CF button cells was measured at several states-of-discharge, after storage under several environments, to assess the reliability of such power sources under very low drain. The internal resistance was measured by the a.c. impedance and galvanostatic pulse methods as a function of storage time at 20 °C, 40 °C/93% RH and 55 °C. For the Li/CF cells, the current level has a significant influence on the total cell impedance determined by the galvanostatic pulse method. The increase of the internal impedance is not only a function of the storage environment due to water permeation through the crimp seal but also of the state-of-discharge. The latter effect may arise from the volume changes which occur during discharge and modify the tightness and permeability of the plastic crimp seal. The total internal impedance of the Li/MnO_2 cells reaches 1 kΩ after 270 days at 40 °C/93% RH and 630 days at 55 °C, while that of the Li/CF cells reaches 1 kΩ after 30 days under both conditions. The storage times extrapolated at an operating temperature of 28 °C are well below the expected value.

1. Introduction

In Part I of this series [1], the passivation resistance and weight change of commercial Li/MnO_2 and Li/CF button cells were measured after storage under several environments to assess the reliability of these power sources, especially that of the plastic crimp seal. It was found that the permeation of the solvent from the electrolyte out of, and of water into the cell occurred simultaneously but at different rates, depending on the environment and type of cell. The plastic crimp seal of the Li/MnO_2 cell exhibited high solvent permeability and low water permeability, whereas the opposite was observed for the Li/CF cell. The main contribution to the increase of the activation resistance was found to be water permeation.

0378-7753/89/$3.50

In this paper the same experimental approach was applied to cells predischarged at different levels to investigate the effect of the state-of-discharge on the increase in the activation resistance, and to predict the useful lifetime of the crimp-sealed lithium cells.

2. Experimental

The type of cells used and the measurement methods were described in Part I of this series [1]. In addition, for each type of cell, four lots, each of six samples, were discharged to 20, 40, 60 and 80% of their initial capacity, determined by discharge into 30 kΩ at 20 °C. At least 16 samples were not discharged; the predischarges were performed into 150 kΩ for a total of about 180 days.

After the partial discharge, each lot of 6 cells was divided into three and stored under the following conditions: (a) 20 °C/60 ± 15% relative humidity (RH); (b) 40 °C/93% RH; (c) 55 °C. The internal resistances of the cells were then measured at regular time intervals.

After 720 days of storage, the resistive discharges were performed, or continued, to check the state-of-discharge of each cell. The resistance values will be given as a function of the initial state-of-discharge, *i.e.*, after the partial discharge, and not after the final state-of-discharge following 720 days of storage. The state-of-discharge refers to the ratio of predischarge capacity to the maximum capacity available from the cell.

3. Results

Examples of the impedance data obtained by both the a.c. and the galvanostatic pulse techniques were reported and discussed in the first part of this series [1].

3.1. Li/MnO$_2$ cells

The variation of the activation resistance, R_{act}, as a function of storage time under three environments is shown in Fig. 1(a) - (c) for several states-of-discharge. After storage at 20 °C (Fig. 1(a)), the activation resistance increased almost linearly with time, from 10 to 25 Ω after the partial discharges to 30 - 85 Ω over 720 days of storage. At 40 °C/93% RH (Fig. 1(b)), the activation resistance increased exponentially with storage time to reach 1 kΩ after 300 days of storage for the undischarged cells and after 540 days for the 20% discharged cells. At 55 °C (Fig. 1(c)), the resistance increase was almost linear for up to about 360 days, then rose more rapidly. It was much smaller than at 40 °C/93% RH. The activation resistance reached a maximum value of 600 Ω at 60% discharge compared with several kΩ in a humid environment.

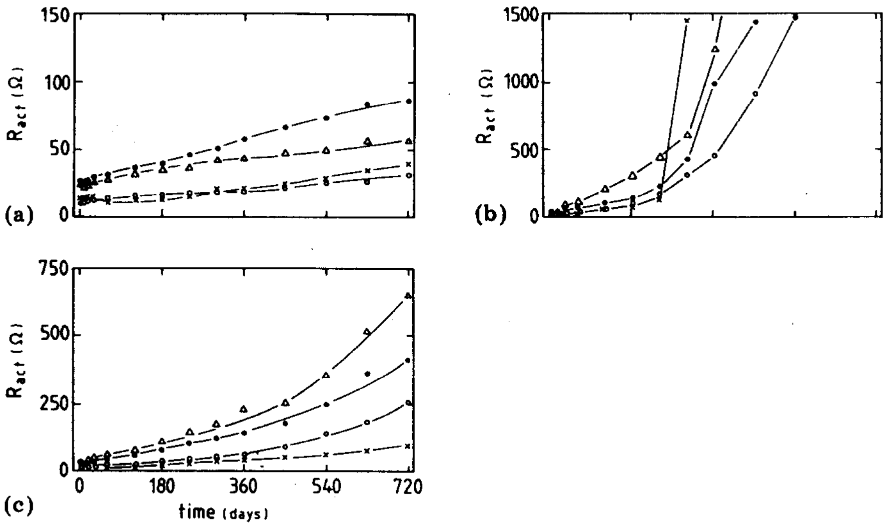

Fig. 1. Dependence of R_{act} on storage time at (×) 0%; (○) 20%; (●) 40%; (△) 60% state-of-discharge for the Li/MnO$_2$ cells stored at 20 °C (a), 40 °C/93% RH (b), 55 °C (c).

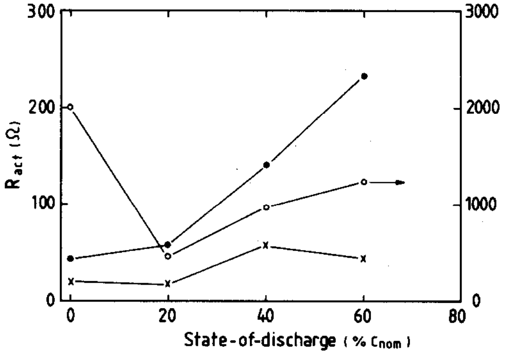

Fig. 2. Dependence of R_{act} on state-of-discharge after 360 days of storage at (×) 20 °C, (○) 40 °C/93% RH, (●) 55 °C for the Li/MnO$_2$ cells.

After storage at 20 °C and at 55 °C, the increase of the activation resistance was higher for the highly discharged state than for the lower states (Fig. 2). At 40 °C/93% RH the undischarged state had the highest R_{act} value, while for states-of-discharge higher than 20% the activation resistance rose with increasing state-of-discharge (Fig. 2).

After storage at 40 °C/93% RH and 55 °C, the series resistance, R_s, increased exponentially with increasing storage times for the highly discharged states, while it remained practically constant for the lower states-of-discharge (Fig. 3(a) and (b)). The various relationships found between R_{act} and R_s (Fig. 4) indicated that both values increased independently of each other. At low states-of-discharge R_{act} increased while R_s remained constant. For the highly discharged states there was one particular relationship

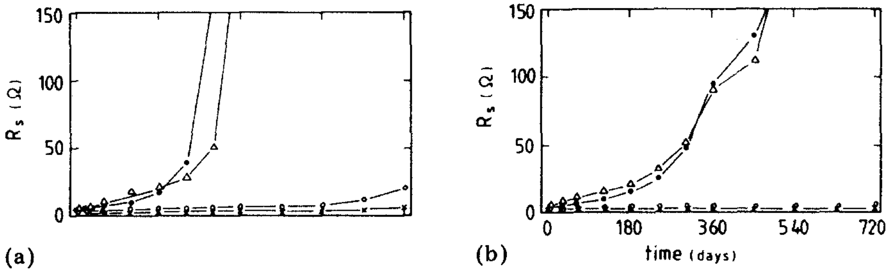

Fig. 3. Dependence of R_s on storage time at (X) 0, (○) 20%, (●) 40%, (△) 60% state-of-discharge for the Li/MnO$_2$ cells stored at 40 °C/93% RH (a) and 55 °C (b).

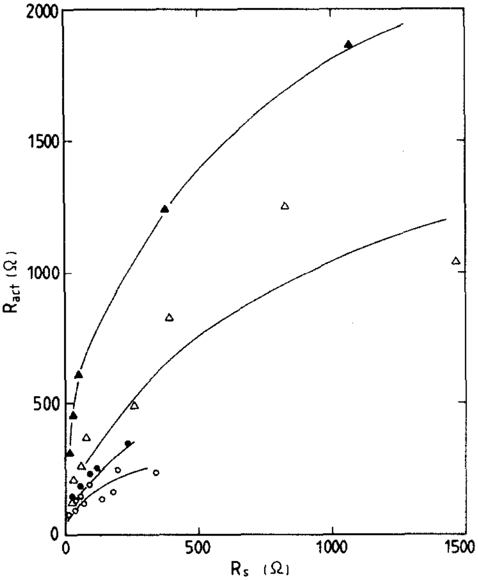

Fig. 4. Dependence of the activation resistance, R_{act}, on the series resistance, R_s, for the Li/MnO$_2$ cells discharged at 40% (open symbols) and 60% (solid symbols) after discharge at 40 °C/93% RH (triangles) and 55 °C (circles).

between R_{act} and R_s for each state-of-discharge and each storage condition. The series resistance was practically constant with storage time at 20 °C.

The galvanostatic pulse method gives the total cell impedance $R_t = R_s + R_{act}$. The data reported in Fig. 5 indicate that when R_s was negligibly small with respect to R_{act}, there was a good correlation between R_{act} given by the a.c. impedance method and R_t given by the galvanostatic pulse technique. After storage at 55 °C, the 40% and 60% discharged cells had a total impedance (Fig. 5(c)) which was roughly the sum of R_{act} (Fig. 1(c)) and R_s (Fig. 3(b)).

The complementary discharges performed after 720 days of storage gave dispersed states-of-discharge (Table 1). The cells stored at 40 °C/93% RH exhibited a final thickness, after the complementary discharge, slightly

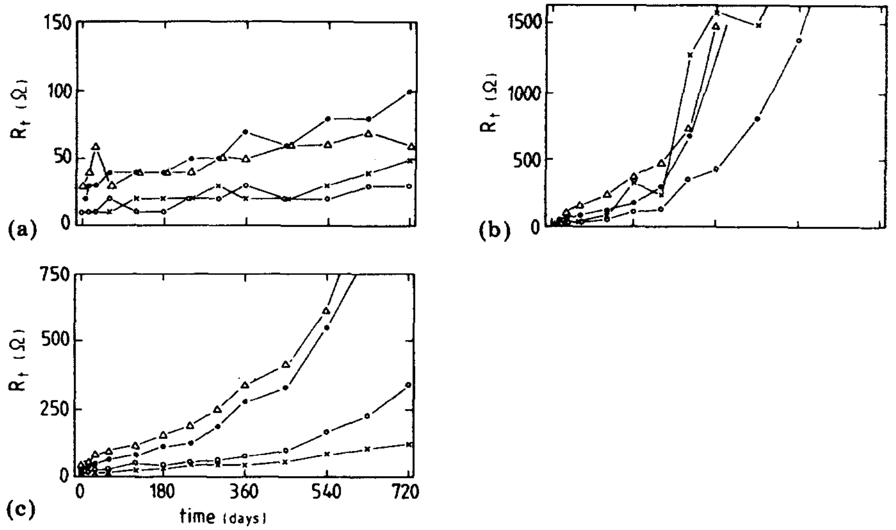

Fig. 5. Dependence of the total cell impedance, R_t, measured by the galvanostatic pulse method (ohmic drop after 10 ms under 0.1 mA) on storage time at (×) 0, (○) 20, (●) 40, and (△) 60% state-of-discharge for the Li/MnO_2 cells stored at 20 °C (a), 40 °C/93% RH (b) and 55 °C (c).

TABLE 1

Final state-of-discharge of the Li/MnO_2 cells after 720 days of storage under three environments

Initial capacity 92 mA h, cut-off 2.0 V, discharged into 30 kΩ.

Initial state-of-discharge (%C_{nom})	Final state-of-discharge (%C_{nom})		
	20 °C	40 °C/93% RH	55 °C
0	1	17	24
	0	17	15
20	19	42	44
	24	38	36
	20	—*	35
	23	36	34
40	50	99	59
	47	98	63
60	42	—*	70
	43	99	69

*Cell leaking before the complementary discharge.

higher than those stored at 20 °C and 55 °C. The thickness depended also on the state-of-discharge for the cells stored at 40 °C/93% RH, while that of those stored at 20 °C and 55 °C was within the experimental scatter (Fig. 6).

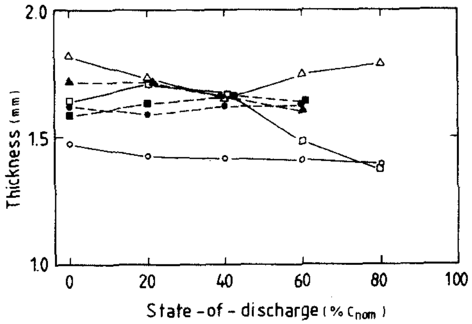

Fig. 6. Final thickness of the Li/MnO$_2$ (solid symbols) and Li/CF (open symbols) cells after the complementary discharge following 720 days of storage at 20 °C (circles), 40 °C/93% RH (triangles) and 55 °C (squares) as a function of the initial state-of-discharge.

3.2. *Li/CF cells*

The activation resistances were significantly higher than those of the Li/MnO$_2$ cells (Fig. 7). After storage at 20 °C, they were between 150 and 600 Ω (Fig. 7(a)), compared with <90 Ω for the Li/MnO$_2$ cells (Fig. 1(a)). At discharged states lower than 40% C_{nom}, R_{act} reached a maximum value after 30 - 180 days, while at 60% - 80% discharge the activation resistance increased linearly to reach a stable value after about 180 - 360 days of storage. At 40 °C/93% RH, R_{act} increased rapidly after short storage times then levelled off between 1 and 2 kΩ for medium states-of-discharge, whereas for the undischarged and 80% discharged cells the activation

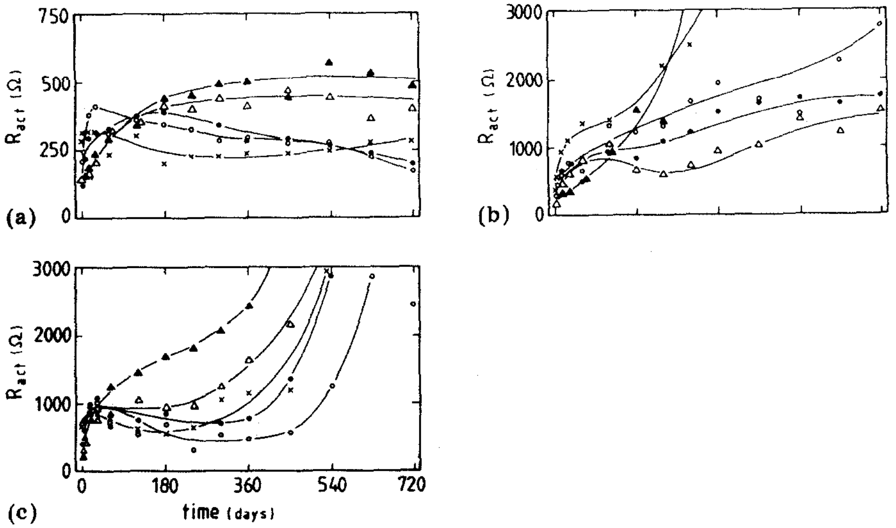

Fig. 7. Dependence of R_{act} on storage time at (×) 0%, (○) 20%, (●) 40%, (△) 60%, and (▲) 80% state-of-discharge for the Li/CF cells stored at 20 °C (a), 40 °C/93% RH (b) and 55 °C (c).

resistance exceeded 3 kΩ after 270 days of storage (Fig. 7(b)). At 55 °C, a sharp increase was again recorded at short storage times, followed by a decrease (with the exception of the 80% discharged state), and a sharp rise (Fig. 7(c)).

The increase in the activation resistance after storage times longer than 360 days at 40 °C/93% RH and 55 °C was higher for the undischarged and highly discharged states than for those between 20% and 60% (Fig. 8).

After storage at 40 °C/93% RH the series resistance, R_s, increased almost linearly with time up to about 400 days from 4 - 5 Ω to 6 - 8 Ω for small states-of-discharge, whereas the rise was exponential for the 60% and 80% discharged cells (Fig. 9(a)). A similar behaviour was measured at 55 °C with a rapid increase of R_s at shorter storage times (Fig. 9(b)). In most cases R_s was very small compared with R_{act}. At 20 °C the increase of R_s with storage time was negligible. As already observed, for the Li/MnO_2 cells, there was no universal correlation between R_{act} and R_s; the relationship depended on the storage conditions and state-of-discharge.

The results obtained with the galvanostatic pulse method were in agreement with those given by the a.c. impedance technique when R_{act} was small, *i.e.*, after storage at 20 °C (Figs. 7(a) and 10(a)). By contrast, when the activation resistance was larger than 500 Ω, *i.e.*, after storage at 40 °C/93% RH and at 55 °C, the total cell impedance, R_t, measured with

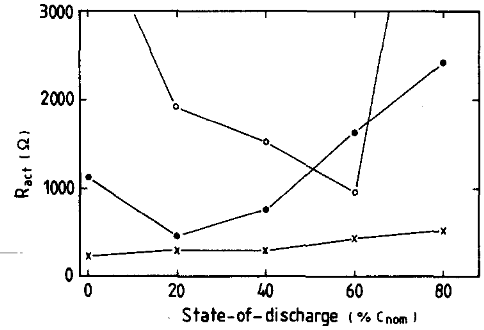

Fig. 8. As Fig. 2 for the Li/CF cells.

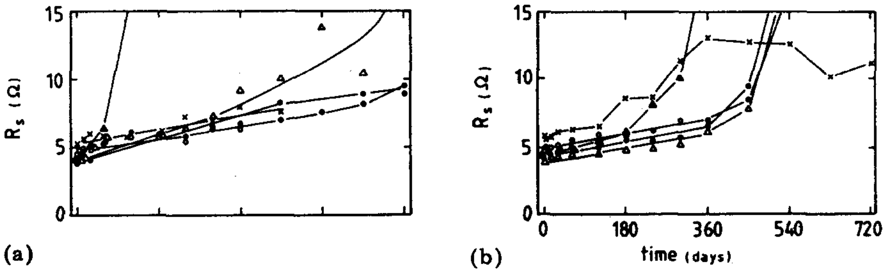

(a) (b)

Fig. 9. Dependence of R_s on storage time at (×) 0%, (○) 20%, (●) 40%, (△) 60%, and (▲) 80% state-of-discharge for the Li/CF cells stored at 40 °C/93% RH (a) and 55 °C (b).

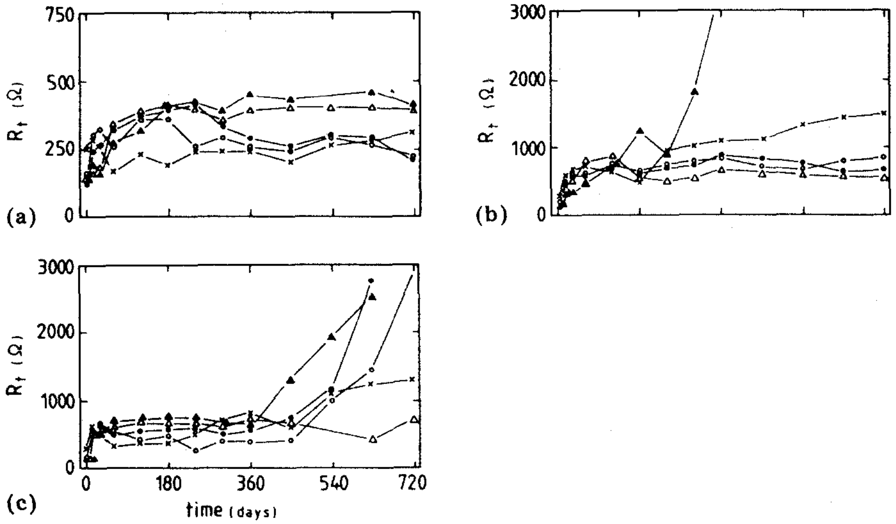

Fig. 10. Dependence of the total cell impedance, R_t, measured by the galvanostatic pulse method (ohmic drop after 10 ms under 0.1 mA) on storage time at (×) 0%, (○) 20%, (●) 40%, (△) 60%, and (▲) 80% state-of-discharge for the Li/CF cells stored at 20 °C (a), 40 °C/93% RH (b), and 55 °C (c).

the galvanostatic pulse method, was significantly smaller than R_{act} determined by the a.c. impedance technique (Figs. 7 (b), (c) and 10 (b), (c)). For example, after storage at 40 °C/93% RH, the cell impedance measured by the galvanostatic method exceeded 1 kΩ only for the 80% discharged cells after 150 days of storage, whereas R_{act} was higher than 1 kΩ after 30 (0% D) to 360 days (60% D).

The complementary discharges performed after 720 days of storage gave homogeneous results (Table 2) from which the following self-discharge over 720 days can be calculated: 1% - 3% C_{nom} (1.6 mA h) at 20 °C; 16% - 25% C_{nom} (16 mA h) at 40 °C/93% RH; 12% - 18% C_{nom} (12 mA h) at 55 °C. The final thickness after the complementary discharges varied significantly with the storage environment and the state-of-discharge (Fig. 6).

4. Discussion

It has been shown that the changes in the internal impedance and weight of Li/MnO$_2$ and Li/CF button cells could be explained by water permeation into, and solvent permeation out of, the cell [1]. The increase in R_{act} is mainly due to water permeation through the plastic crimp seal. In the following section, the effect of the state-of-discharge and environment will be discussed and an attempt will be made to predict the useful lifetime for a given application.

The increase in the activation resistance of standard commercial 2/3 A size Li/CF cells with time after discharge at ambient temperature has already

TABLE 2

Final state-of-discharge of the Li/CF cells after 720 days of storage under three environments

Initial capacity 78 mA h, cut-off 2.0 V, discharged into 30 kΩ.

Initial state-of-discharge (%C_{nom})	Final state-of-discharge (%C_{nom})		
	20 °C	40 °C/93% RH	55 °C
0	1	25	12
	0	22	12
20	21	41	37
	22	36	38
40	42	59	93
	43	60	72
60	62	77	72
	62	76	71
80	84	100	99
	83	100	98

been found to change with the state-of-discharge [2]. The cell construction and, probably, the electrolyte composition were different from those used in the cells of the present study [2, 3].

For the Li/CF cells stored at 40 °C/93% RH and 55 °C, the current has a significant effect on the total cell impedance measured by the galvanostatic pulse method. This means that a high current can break down the passivation layer and decrease the internal resistance. Under these circumstances, the time required to reach a given resistance will depend on the current drain.

4.1. *Activation energies*

Typical activation energies will be estimated from the variation of the activation resistance, R_{act}, with temperature under two conditions: first, between 20 °C and 55 °C, where it is assumed that the humidity plays a small role, and second, between 20 °C and 40 °C/93% RH where the effect of humidity is predominant. Unfortunately, the humidity was not constant at the various temperatures. The activation energies resulting from the difference in R_{act} values measured at 20 °C/60% RH and 40 °C/93% RH are expected to be higher than those that would be obtained at constant RH.

The data in Fig. 11 and Table 3 show that the activation energy of permeation, E_p, depends on the storage time, on the storage environment, and, to a lesser extent, on the state-of-discharge. The activation energy increases with storage time. For the Li/MnO_2 cells, it is significantly higher in wet atmospheres than in dry media, while for the Li/CF cells the values calculated between 20 °C and 40 °C are not always larger than those between 20 °C and 55 °C. The 60% discharged Li/CF cells have the same E_p in the

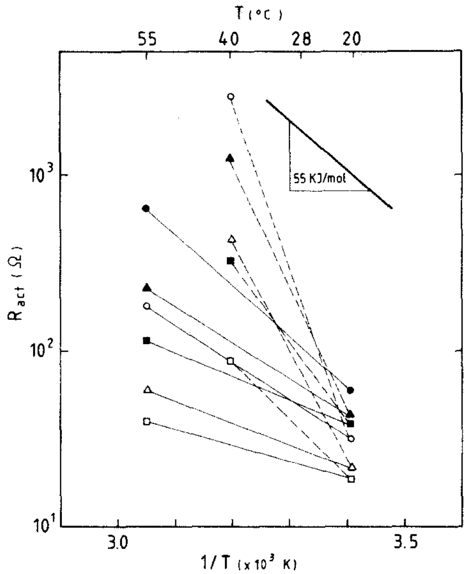

Fig. 11. Temperature dependence of R_{act} for the Li/MnO$_2$ cells 180 (squares), 360 (triangles) and 720 (circles) days after discharge at 20% (open symbols) and 60% C_{nom} (solid symbols).

TABLE 3

Typical activation energies estimated from the differences in R_{act} between (i) 20 °C and 40 °C/93% RH; (ii) 20 °C and 55 °C

State-of-discharge (%C_{nom})	Storage time (days)	E_p (kJ mol^{-1})	
		20 - 40 °C/93% RH	20 - 55 °C
Li/MnO$_2$ cells			
20	180	61	17
	360	116	23
	720	195	40
60	180	84	25
	360	147	38
	720	209	55
Li/CF cells			
20	180	48	16
	360	72	12
	720	100	~70
60	180	21	19
	360	33	32
	720	~53	~53

entire temperature range. Such a complex behaviour of the activation energy has already been discussed for the undischarged state [1].

In the case of the Li/CF cells, the activation energies calculated from the resistances determined by the galvanostatic pulse method at low current are smaller (*i.e.*, 10 - 50 kJ mol^{-1} between 20 °C and 40 °C/93% RH and about 10 kJ mol^{-1} between 20 °C and 55 °C) than those estimated from R_{act} measured by the a.c. impedance technique (Table 3).

With so many parameters involved, the predicted lifetime at low temperature from values measured at high temperature must be considered with caution.

4.2. Estimated lifetime for a given application

As an example of a typical application, the operation of a man's wrist-watch will be considered. Using the latest technologies, the total cell impedance at ambient temperature should be smaller than 1 kΩ to keep the watch running. At higher impedance values, the ohmic drop would be too large and the oscillator or stepping motor would cease to work. It will further be assumed that the wrist-watch is constantly worn and that its temperature is 28 °C.

Under normal operating conditions, the current (about 1 μA) drawn by the watch is too low to break down the passivation layer on the lithium electrode. Under the experimental conditions of the present study, *i.e.*, storage without any current drawn from the cell, the growth of the passivation layer is expected to be amplified with regard to the operation under very low drain.

The estimation of the lifetime, characterized by the storage time required to reach a total impedance of 1 kΩ, will be done as follows. As the increase of resistance depends on the state-of-discharge, the two extreme cases will be considered. The minimum and maximum storage times required to reach 1 kΩ, and the state-of-discharge at which they correspond for both 40 °C/93% RH and 55 °C, are given in Table 4. The activation energy was then calculated for each test condition and each state-of-discharge at the time considered or at a time slightly shorter than the sharp rise of resistance (see, *e.g.*, Fig. 1(b)). The acceleration factor between the test temperature and 28 °C was then calculated from E_p. The storage time at 28 °C was finally estimated by multiplying the storage time at the test temperature by the acceleration factor (Table 4).

4.2.1. Li/MnO$_2$ cells

In a humid environment (40 °C/93% RH), the R_{act} of the Li/MnO_2 cells reached 1 kΩ after 270 (undischarged state) to 450 days (20% discharged) (Fig. 1(b)). Using the acceleration factors calculated at the corresponding state-of-discharge and storage environment, a storage time between 810 and 2250 days was estimated at 28 °C (humid), depending on the state-of-discharge (Table 4).

TABLE 4

Minimum and maximum storage times estimated at 28 °C from the acceleration factors calculated from R_{act} between the test temperature and 28 °C for two test environments

Test conditions	Storage time at T_{test} for R_{act} = 1 kΩ (days)	State-of-discharge (%C_{nom})	Acceleration factor between T_{test} and 28 °C	Storage time at 28 °C for R_{act} = 1 kΩ (days)
Li/MnO$_2$ cells				
40 °C/93% RH	270	0	3	>810
	450	20	5	<2250
55 °C	630	40 - 60	4	>2520
	>720	0 - 20	4	>2880
Li/CF cells				
40 °C/93% RH	30	0	2	>60
	360	60	2	<720
55 °C	30	80	3	>90
	540	20	3	<1620

The Li/MnO$_2$ cells stored at 55 °C for 720 days after discharge at 40% and 60% exhibited R_{act} and R_s of roughly the same value (Figs. 1(c) and 2(b)). The total cell impedance for these two states-of-discharge was higher than 1 kΩ after about 630 days. At smaller states-of-discharge, the series resistance R_s was negligibly small and the R_{act} was well below the critical 1 kΩ value. Using the acceleration factor calculated at the corresponding state-of-discharge and storage environment (Table 4), a storage time larger than 2520 days was estimated at 28 °C (dry).

4.2.2. Li/CF cells

After storage at 40 °C/93% RH, the activation resistance of the Li/CF cells reached 1 kΩ after 30 (undischarged state) to 360 days (60% discharged) (Fig. 7(b)), while the total cell impedance measured by the galvanostatic method reached 1 kΩ after 240 (0% and 80% discharge) to >720 days (20% - 60% discharge) (Fig. 10(b)). Using the acceleration factor calculated at the corresponding state-of-discharge and storage environment (Table 4), a storage time between 60 and 720 days is estimated at 28 °C (humid) from the R_{act} values determined by the a.c. impedance technique (very low drain). The R_{act} values measured by the galvanostatic method indicate that the storage time at 28 °C (humid) could be larger than 480 days if the current is high enough to break down the passivation layer.

After storage at 55 °C, R_{act} measured by the a.c. method (very low drain) reached 1 kΩ after 30 (80% discharge) to 540 days (20% discharge) (Fig. 7(c)), indicating a storage time of 90 to 1620 days at 28 °C (dry). The galvanostatic method (high drain) gave 450 days to reach 1 kΩ at 80%

discharge and more than 720 days at 60% discharge (Fig. 10(c)), indicating an estimated storage time at 28 °C (dry) larger than 1350 days (Table 4).

4.3. Self-discharge and thickness change

The self-discharge of lithium cells, which arises mainly from the reaction of the lithium electrode with impurities, is expected to be mainly related to the lithium area and not to its volume. Thus, the self-discharge should be independent of the state-of-discharge during storage. The amount of water which permeates through the plastic seal, however, depends not only on the storage environment but also on the state-of-discharge. The data collected in Table 2 indicate that the latter effect is difficult to distinguish from the scatter of the measurements. It is interesting to note that, under the most severe environment, the self-discharge is comparable with the power consumption of a watch.

The influence of the state-of-discharge on the increase in the internal resistance may be explained by the volume changes which occur during discharge. The final thickness of the cell depends on the storage environment and on the state-of-discharge. The effects are especially worth noting for the Li/CF cells (Fig. 6). The increase related to the humidity in the storage environment has already been discussed relative to the undischarged cells [1]. The changes induced on the plastic seal by the environmental conditions come in addition to the volume changes which take place during the pre-discharge. The variations of the volume of the electrode components may result in significant mechanical stresses on the crimp seal. Such an effect may strongly modify the tightness and permeability of the seal and consequently change the internal resistance of the cell. Repeated cooling and heating of the cells for the measurements might also have contributed to the development of leaks by expansion and contraction in some of the Li/MnO_2 cells (see Table 1).

5. Conclusions

The results of the present study show that the storage and, by extension, the use at very low drain, of the Li/MnO_2 and Li/CF button cells increase the internal impedance, especially under humid environment (40 °C/ 93% RH). The increase of R_{act} is also a function of the state-of-discharge. The latter effect is believed to arise from the volume changes which occur during discharge modifying the tightness and permeability of the crimp seal.

The lifetime of the CR 2016 Li/MnO_2 cell at the more sensitive state-of-discharge, based on the assumption that the internal impedance at ambient temperature should be smaller than 1 kΩ, would be about 270 days at 40 °C/93% RH and 630 days at 55 °C. That of the BR 2016 Li/CF cell would be only 30 days under both environments. There are too many parameters involved to predict a precise lifetime at the working temperature of a wrist-watch, *i.e.*, 28 °C, on the basis of the accelerated tests. The approximate storage times obtained are, however, well below the expected value of 8 years (2880 days) claimed by the manufacturer [3].

For applications where the estimated lifetime is longer than 3 - 5 years, it would be advisable to use hermetically sealed cells, *i.e.*, with glass-to-metal or ceramic-to-metal feedthroughs. Unfortunately such cells, small enough for watches and other low power consumption devices, are not yet commercially available, although the need has already been stressed [4].

The main advantage of lithium cells is their long shelf life. These cells are best used in applications where the power consumption is low and, consequently, the current very small. The passivation of the lithium electrode occurs especially under these very conditions. Thus, the crimp-sealed lithium cells have paradoxical properties. To avoid the future of the lithium cells being compromised by the very qualities which should assure their success, the manufacturers should introduce the hermetic seal, especially for applications where the environment is hot and humid.

Acknowledgements

The author is pleased to thank F. Züllig for his skillful assistance in the experimental work, R. Jeanmonod for discharge measurements, and ETA Inc., Grenchen, member of SMH Group, for its interest and support. A summary of this work was presented at the 174th Meeting of The Electrochemical Society, Chicago, IL, Oct. 11, 1988, and will be published in a proceedings volume of this society.

List of symbols

R_s	Series resistance (electrolyte, separator, current collectors and leads' resistance) defined in the complex plane as the high-frequency intercept of the real axis
R_{act}	Activation resistance defined in the complex plane as the diameter of the semi-circle
R_t	Total cell impedance ($R_t = R_s + R_{act}$)
Re	Real part of the impedance
Im	Imaginary part of the impedance
E_p	Activation energy of permeation

References

1 J. P. Randin, *J. Power Sources, 25* (1989) 49.
2 J. R. Sandifer and M. R. Suchanski, *J. Appl. Electrochem., 14* (1984) 329 - 340.
3 M. Fukuda and T. Iijima, in J. P. Gabano (ed.), *Lithium Batteries*, Academic Press, London, 1983, pp. 211 - 239.
4 S. C. Levy, *J. Power Sources, 20* (1987) 353.